

Supporting Information

Hierarchical Cu-MOF Hollow Nanowires Modified Copper Mesh for Efficient Antibacterial PM Filtration

Haiyan Li,^a Tao Wang,^{a,} Yulong Ying,^a Zhiqi Wang,^a Lianjun Pan,^b and Sheng
Wang^{a,*}*

*^aSchool of Materials Science and Engineering, Zhejiang Sci-Tech University,
Hangzhou 310018, China*

*^bZhejiang Light Industrial Products Inspection And Research Institute, Hangzhou
310000, China*

E-mail address of the corresponding author:

Tao Wang: wangtao@zstu.edu.cn; taotao571@hotmail.com;

Sheng Wang: wangsheng@zstu.edu.cn; wangsheng571@hotmail.com

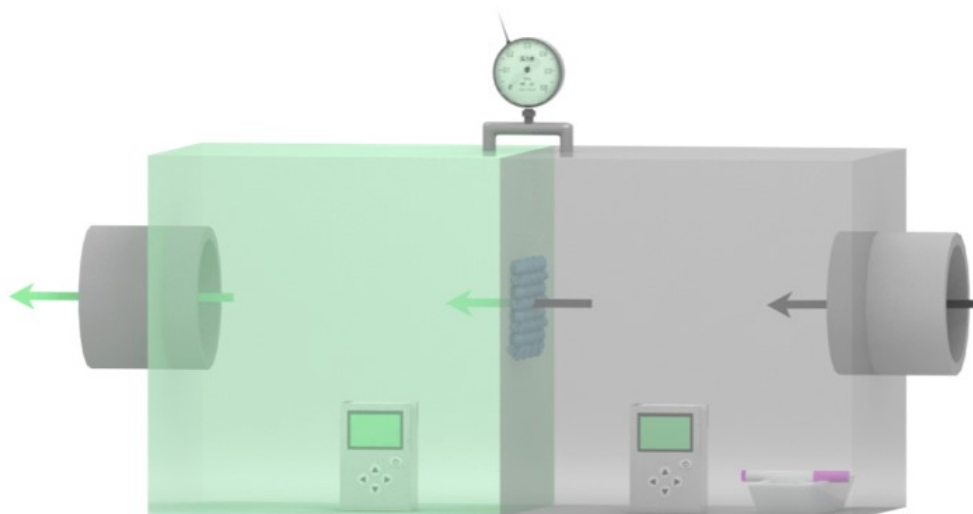


Figure S1. Home-made smoke tester for PM particles capture process.

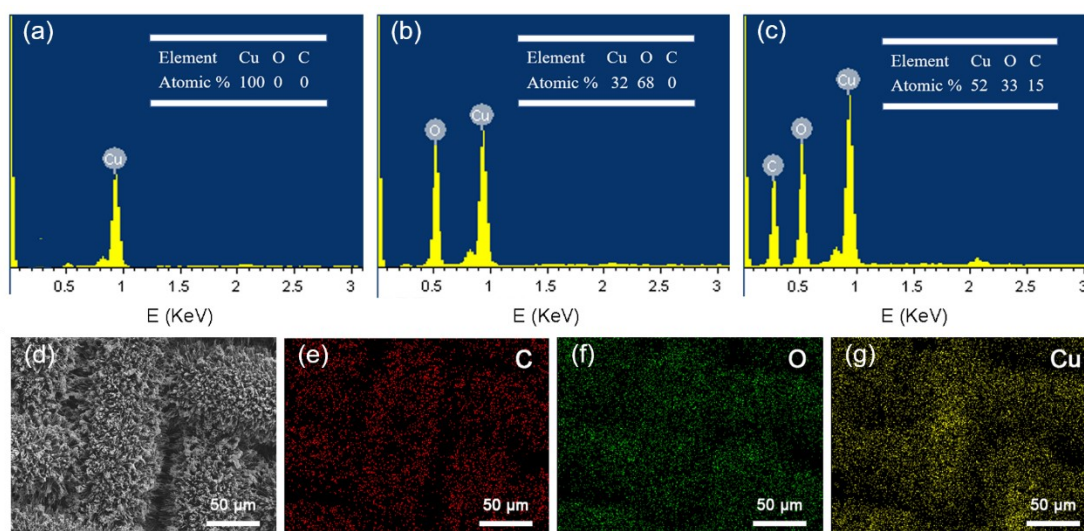


Figure S2. EDX spectra of the products obtained at different reaction processes. (a) pristine copper mesh, (b) CHM, and (c) CMM-70. (d) SEM image and EDS mapping of (e) C, (f) O, and (g) Cu elements of CMM-70.

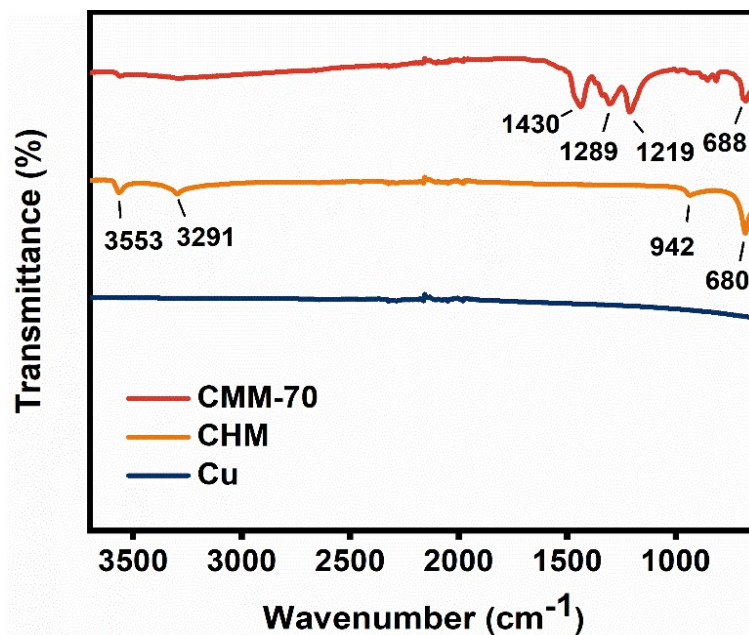


Figure S3. FTIR of the products obtained at different reaction processes, pristine copper mesh, CHM, and CMM-70.

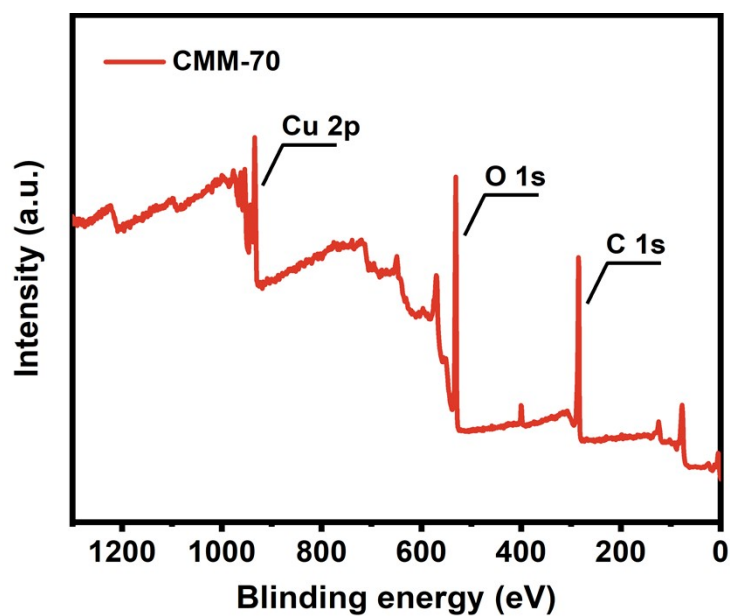


Figure S4. Survey spectrum of CMM-70.

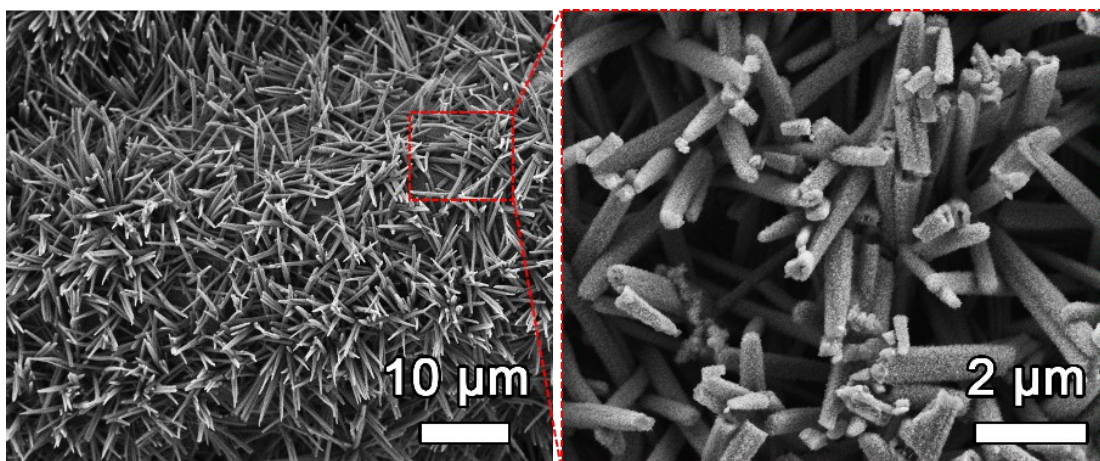


Figure S5. CMM-90 nanometer array partially collapsed surface morphology.

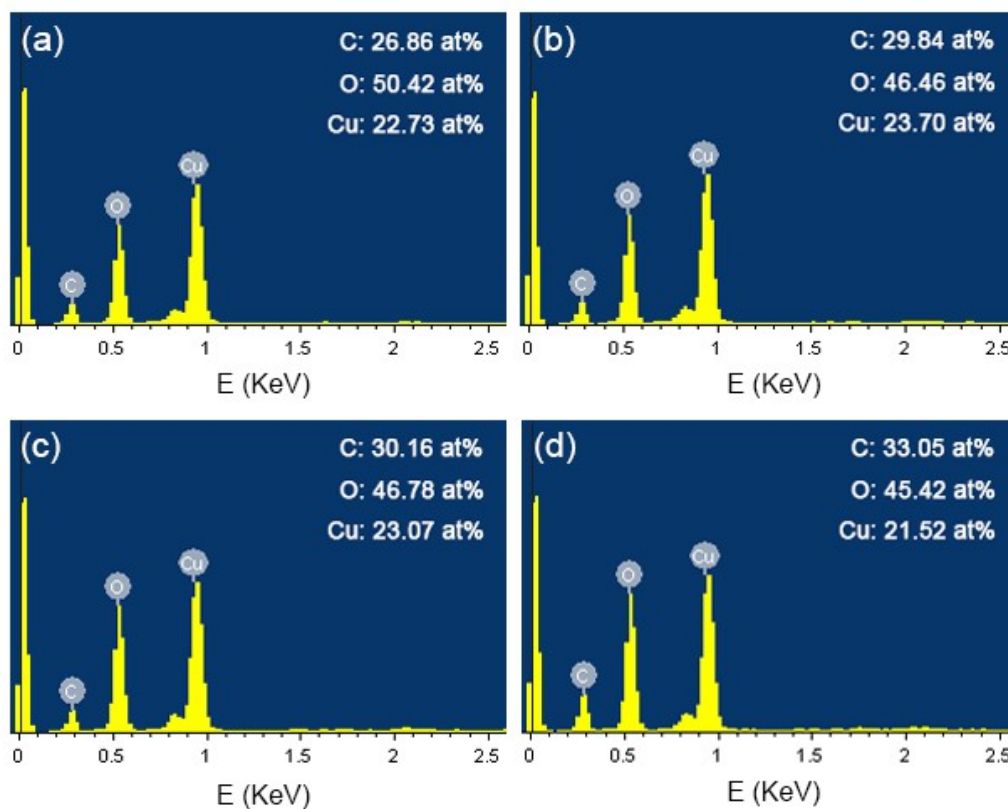


Figure S6. EDX spectra of modified mesh samples obtained at different reaction temperature: (a) Cu-MOF-30, (b) Cu-MOF-50, (c) Cu-MOF-70, and (d) Cu-MOF-90.

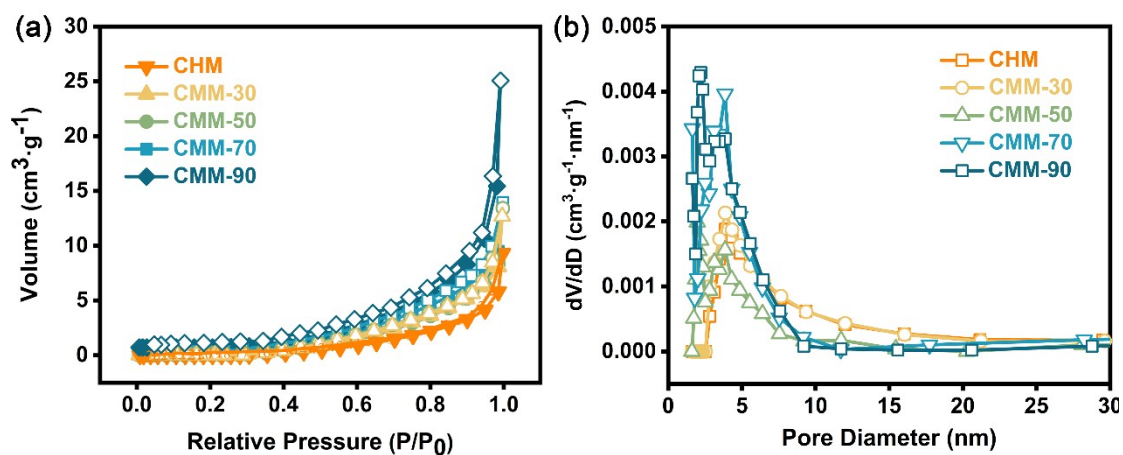


Figure S7. (a) Nitrogen adsorption–desorption isotherms and (b) pore size distributions of the modified copper meshes.

Table S1. The BET-specific surface area of the modified copper meshes.

Sample	S_{BET} (m ² /g)
Copper mesh	/
CHM	5.13
CMM-30	9.19
CMM-50	15.52
CMM-70	25.34
CMM-90	22.53

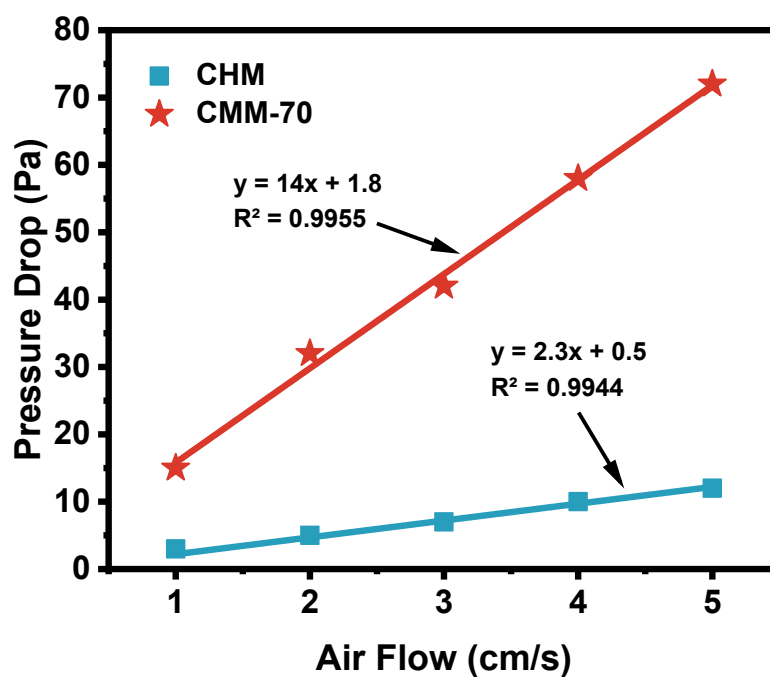


Figure S8. The pressure drop of the mesh samples under different airflow rates.

Table S2. Comparison of comprehensive PM_{2.5} and PM₁₀ filtration performance of filters via home-made smoke tester at the air flow rate 0.2 m s⁻¹.

PM	Filter	E ^a (%)	ΔP ^b (Pa)	Q ^c (Pa ⁻¹)
PM _{2.5}	Copper mesh	20.1	1	-
	CHM	78.8	32	0.048
	CMM-30	92.2	36	0.071
	CMM-50	93.5	38	0.072
	CMM-70	96.0	36	0.089
	CMM-90	92.8	39	0.067
PM ₁₀	Copper mesh	21.3	2	-
	CHM	80.5	34	0.048
	CMM-30	94.1	38	0.074
	CMM-50	95.7	39	0.081
	CMM-70	98.5	37	0.113
	CMM-90	94.3	40	0.072

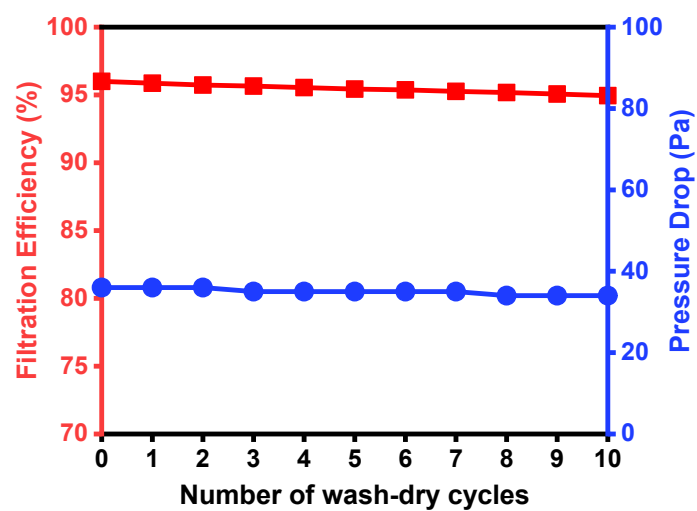


Figure S9. PM_{2.5} filtration efficiency and pressure drop of the CMM-70 filter after ten filtration–wash–dry cycles.

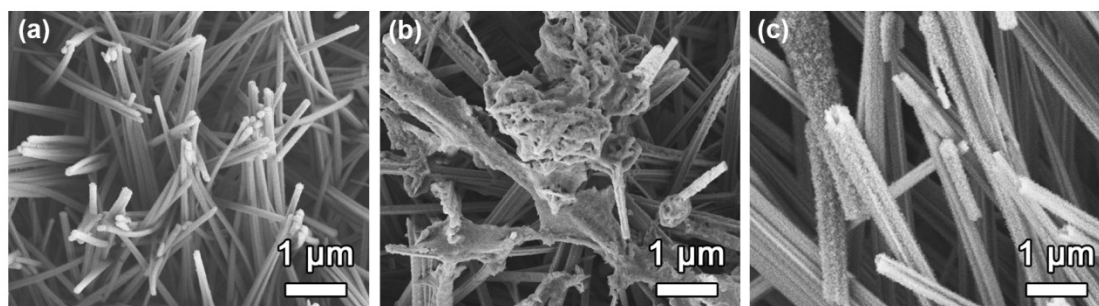


Figure S10. SEM images of CMM-70 (a) Before filtration, (b) after filtration, and after ten filtration–wash–dry cycles.

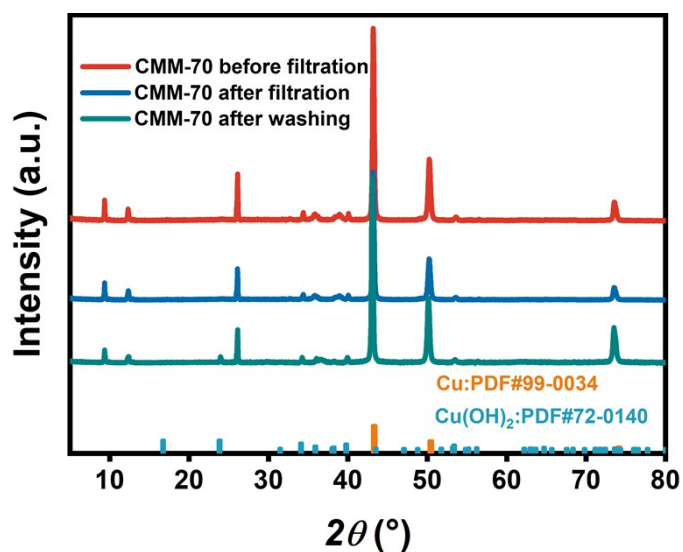


Figure S11. XRD pattern of CMM-70 (a) Before filtration, (b) after filtration, and after ten filtration–wash–dry cycles.

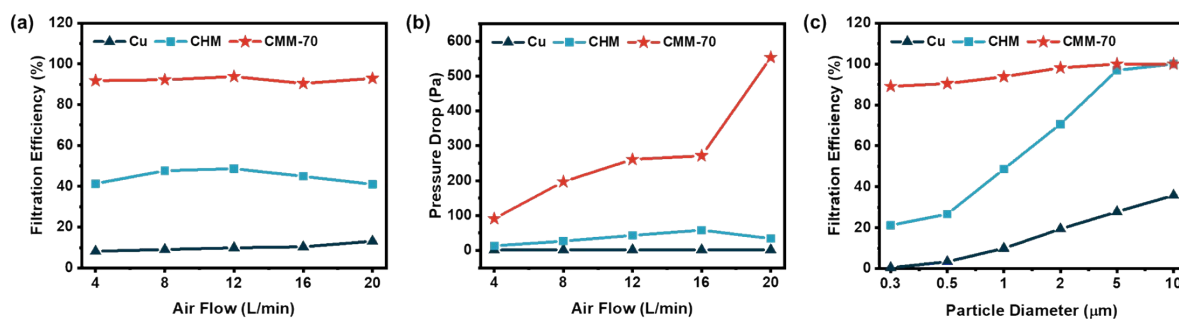


Figure S12. Filtration performance of the cooper mesh, CHM, CMM-70 filters: (a) relationship between airflow rate and filtration efficiency. (b) relationship between airflow rate and pressure drop. (c) Relationship between particle size and filtration efficiency at airflow rate of 12 L/min.

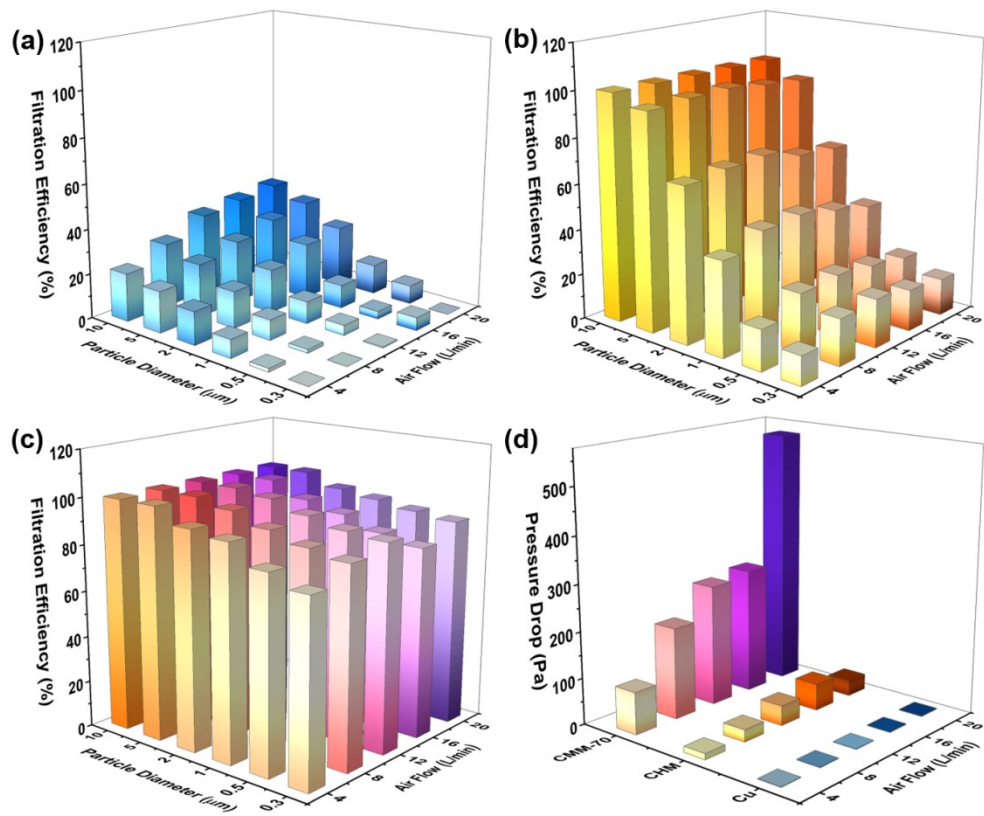


Figure S13. Filtration performance of the cooper mesh, CHM, CMM-70 filters.

Table S3. Comparison of comprehensive PM filtration performance of filters via commercial filtration system.

Filter mesh	Air flow (L/min)	Pressure drop (Pa)	0.3 (μm)	0.5 (μm)	1 (μm)	2.5 (μm)	5(μm)	10(μm)
Copper mesh	4	1	0.00	1.56	8.22	14.82	18.47	21.46
	8	1.5	0.00	4.49	9.07	16.46	23.78	28.39
	12	1.5	0.46	3.39	9.90	19.38	27.78	35.84
	16	1.5	5.77	8.20	10.37	24.76	32.05	37.62
	20	1.5	0.00	10.70	13.13	26.48	34.65	37.65
CHM	4	13	12.69	17.96	41.33	68.05	95.26	100
	8	26.5	20.18	25.71	47.69	69.89	96.53	100
	12	43	21.18	26.67	48.65	70.65	96.91	100
	16	58	18.074	24.14	44.94	66.07	94.70	100
	20	34	16.12	21.32	40.99	64.50	93.18	100
CMM-70	4	91	78.45	83.50	91.79	93.66	100	100
	8	197	85.44	88.10	92.18	97.00	100	100
	12	261	89.11	90.42	93.79	98.14	100	100
	16	271.5	82.20	85.24	90.37	93.85	100	100
	20	553.3	88.85	90.55	92.89	94.96	100	100

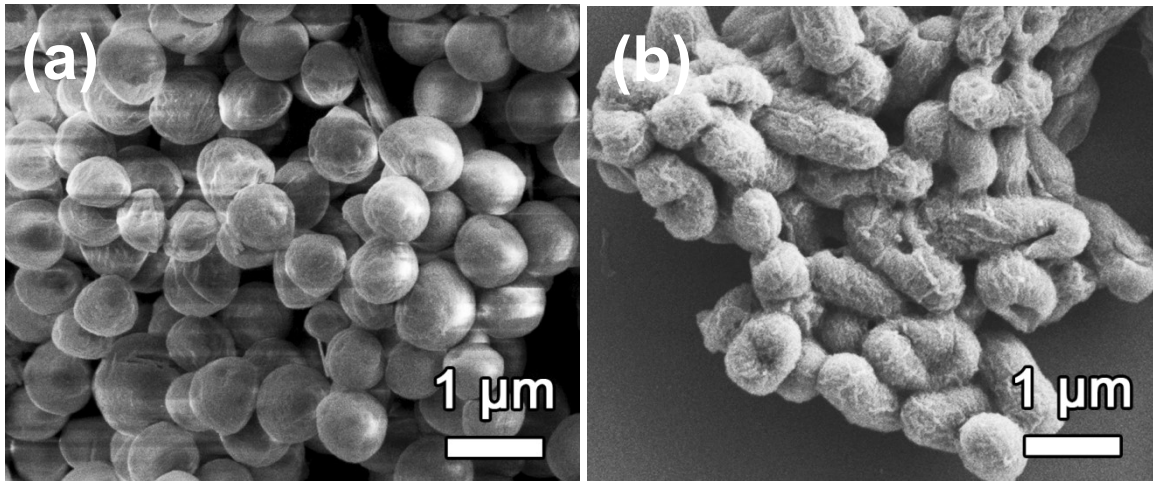


Figure S14. Morphologies of (a) *S. aureus* and (b) *E. coli* after antibacterial treatments.